LA AGUADITA TRACHYTE: NEW EXPONENT OF TRIASSIC ALKALINE MAGMATISM IN SIERRA DE VALLE FÉRTIL, WESTERN SIERRAS PAMPEANAS

Brígida CASTRO de MACHUCA[1,2], María Gimena LÓPEZ[1,2], Diego MORATA[3], Alicia CONTE-GRAND[1], Sandra PONTORIERO[1]

[1] Instituto de Geología, Facultad de Ciencias Exactas, Físicas y Naturales, Universidad Nacional de San Juan, San Juan.
E-mail: bcastro@unsj-cuim.edu.ar
[2] CIGEOBIO-CONICET
[3] Departamento de Geología y Centro de Excelencia en Geotermia de los Andes (CEGA, FONDAP-CONICYT), Facultad de Ciencias Físicas y Matemáticas, Universidad de Chile, Santiago, Chile.

RESUMEN

La Aguadita Trachyte, in Sierra de Valle Fértil, is a new outcrop referring to the Triassic alkaline magmatism. The trachyte body was emplaced along a NNW-trending fault zone overlying the crystalline basement. The trachyte consists mainly of anorthoclase and sanidine as pheno- and microphenocrysts, with lesser amounts of arfvedsonite and ferro-eckermannite in the groundmass. It is moderately evolved in composition with 66.5-69.1 wt.% SiO_2 and exhibits a limited compositional range in most of the major elements. The rare earth elements (REE) pattern is somewhat uniform and highly fractionated, being enriched in light REE over heavy REE and showing a prominent negative Eu anomaly. The trachyte is enriched in high field strength elements Nb, Zr, and Y, consistent with typical intraplate alkaline magmatism associated with continental rifting. It is proposed to be genetically linked to other alkaline volcanic rocks outcropping in the area, and generated from the same parental source (i.e., asthenospheric mantle source) through open-system fractional crystallization. εNd values of +2.6 are consistent with slightly crustal contamination during trachyte generation. Thus, La Aguadita Trachyte could be the result of a combination of fractional crystallization of mantle-derived basaltic magma and crustal assimilation. Radiometric age dating of 218 ± 7 Ma on the trachyte (K-Ar age, whole rock) expands the range of the alkaline volcanism known in the area to the Upper Triassic, and confirms a regional volcanic event related to uplift in an extensional tectonic environment.

Palabras clave: Trachyte, geochemistry, petrogenesis, Upper Triassic, intraplate continental rifting

ABSTRACT

Traquita La Aguadita: Nuevo exponente del magmatismo alcalino triásico en la Sierra de Valle Fértil, Sierras Pampeanas Occidentales
La Traquita La Aguadita, en la Sierra de Valle Fértil, es un nuevo afloramiento del magmatismo alcalino triásico. Se dispone sobre el basamento cristalino y su emplazamiento estuvo controlado por una falla de dirección NNO. La traquita está compuesta principalmente por feno y microfenocristales de anortoclasa y sanidina, con cantidades subordinadas de arfvedsonita y ferro-eckermannita en la mesostasis. Es moderadamente evolucionada en composición con 66,5-69,1 % de SiO_2 y exhibe un rango composicional restringido para la mayoría de los elementos mayoritarios. El patrón de distribución de los elementos de tierras raras (REE) es uniforme y altamente fraccionado, con enriquecimiento de las LREE respecto de las HREE, y prominente anomalía negativa de Eu. La traquita está enriquecida en elementos de alto potencial iónico como Nb, Zr e Y, congruente con magmatismo alcalino de intraplaca asociado a rifting continental. Se propone su vinculación genética con otras rocas volcánicas alcalinas aflorantes en el área, y su generación a partir de la misma fuente primaria (manto astenosférico) mediante cristalización fraccionada. Los valores de εNd = +2.6 son consistentes con un cierto componente de contaminación cortical. De este modo, la Traquita La Aguadita sería resultado de la cristalización fraccionada de magma basáltico derivado del manto combinado con asimilación cortical. La edad radimétrica de 218 ± 7 Ma (K-Ar en roca total) expande el alcance del magmatismo alcalino conocido en el área hasta el Triásico superior, y confirma el carácter regional de este evento volcánico relacionado con la tectónica extensional imperante.

Keywords: Traquita, geoquímica, petrogénesis, Triásico Superior, rift intraplaca continental

INTRODUCTION

In Sierra de Valle Fértil, Western Sierras Pampeanas, a wide variety of alkaline volcanic rocks ranging from olivine alkali-basalt, basaltic trachyandesite, phonolite, trachyte to alkali rhyolite, intrude through and erupt over the crystalline basement of Lower Palaeozoic age (Mirré 1976). The alkaline volcanic suite was mostly emplaced along fractures or pre-existing lithospheric weakness zones (Uliana and Biddle 1988, Ramos and Kay 1991). Most outcrops are located within and on both margins of the NNW-trending Río del Potrero depression extending from Estancia Quiroga in the north to Los Bretes-Los Molles localities in the
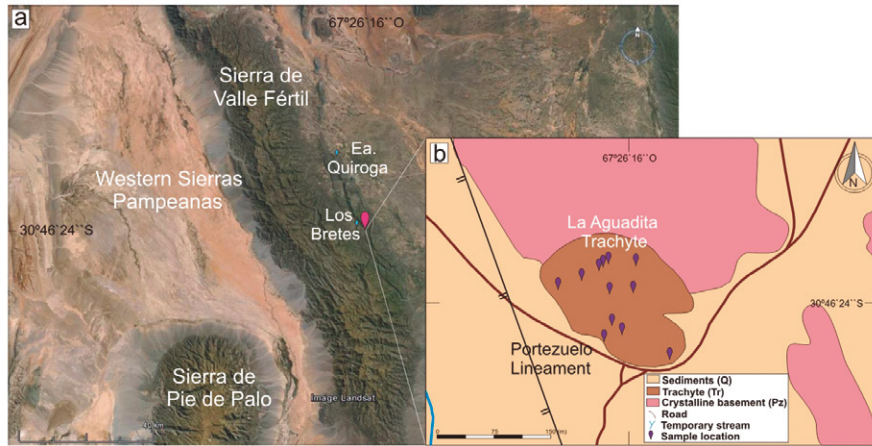
Figure 1: a) Satellite image (from Google Earth 2013) showing the location of La Aguadita Trachyte in Sierra de Valle Fértil, Western Sierras Pampeanas; b) Schematic geologic map of the trachyte outcrop with sample locations.

south (Fig. 1a).

Exposures are poor and occur scattered over the basement within an area of less than 500 km², showing that the igneous activity was volumetrically a subsidiary event though significant in the geotectonic evolution of the region. The geology of these volcanic rocks is not well known; the only study dealing with the volcanism of the area is due to Mirré (1976), who grouped these lithologies as part of a non-orogenic continental alkaline association of uncertain Triassic age. However, detailed petrological investigations on these volcanic rocks are still absent.

Based on petrographic and geochemical similarities with continental alkaline basalts and related rocks from the nearby triassic Ischigualasto-Villa Union basin (San Juan and La Rioja provinces), the alkaline rocks from Sierra de Valle Fértil were included in the Baldecitos Formation and referred to the Middle Triassic by Limarino et al. (2008 and references therein). Radiometric age data (K/Ar and Ar/Ar methods) from basalts interlayered and/or overlying the sedimentary sequence that infilled the Ischigualasto-Villa Union Basin, are constrained between 231 ± 4 Ma and 215 ± 5 Ma (Limarino et al. 2008, Curriea et al. 2009, Martinez et al. 2011, and references therein). These ages indicate a significant magmatic activity concentrated at the base of the Upper Triassic.

The petrology of basaltic rocks from the Baldecitos Formation and lavas of similar composition outcropping in the surroundings has been studied by Page et al. (1997). According to these authors the magmatic series extends from basalt to trachybasalt to trachyte, and was originated under high pressure and temperature conditions involving the fractionation of olivine, ulvöspinel, ilmenite, clinopyroxene, An-rich plagioclase and apatite. The alkaline volcanic rocks seem to be derived from a common source, but basaltic melts were originated separately representing different mantle-melting degrees from source. The resulting rocks are interpreted as being the product of fast magmatic ascent and subsequent intrusion or flow. Temporary storage in smaller chambers at intermediate depth could have been the mechanism for the differentiation process (Page et al. 1997). The present study outlines the petrological, mineralogical, geochemical and isotopic characteristics of an outcrop of volcanic rock named La Aguadita Trachyte *(nov. nom.),* first recognized by Castro de Machuca et al. (2012), and discusses its petrogenetic implications. Data obtained will allow to reconstruct the evolution of this lithology and the tectonic setting of emplacement.

GEOLOGIC SETTING

The Valle Fértil Complex (Cuerda et al. 1984) that make up Sierra de Valle Fér-til, is composed of medium-pressure upper amphibolite to granulite facies metasedimentary rocks (0.6 ± 0.1 GPa, 800 ± 40 °C), predominantly sillimanite-garnet (±cordierite) migmatitic gneisses of Middle to Late Cambrian age, and minor metacarbonates and calc-silicate rocks of unknown age (Casquet et al. 2012 and references therein). During the Famatinian orogeny (Ordovician) voluminous bodies of gabbro, diorite, tonalite, granodiorite and granite, largely concordant with foliation of the host rocks, intrude the metamorphic basement. Field relations suggest that metagabbros are the oldest intrusive rocks with metatonalites, granodiorites and granites being slightly younger (Otamendi et al. 2009 and references therein). Magmatism and metamorphism here took place within a narrow timespan at *ca.* 470 Ma (Casquet et al. 2012 and references therein).

Since the Lower Triassic, the already uplifted Sierra de Valle Fértil (Mirré 1976, Otamendi et al. 2009) experienced an extensive system of north-northwest striking, and continental-rift basins were developed to the north (Ischigualasto-Villa Unión basin) and to the south (Marayes-El Carrizal basin). Transtension was responsible for the main NNW to NW-trending fractures and conjugated NNE to NE-fractures -whose orientation is possibly controlled by the basement structure-, and the subsequent formation of the sedimentary basins (Page et al. 1997 and references therein). During the Mesozoic and Palaeogene the whole area has been exposed to strong erosion (Limarino et al. 2008).

The structure of Sierra de Valle Fértil is the result of several overimposed tectonic deformational events. It is made up of two main components: a complex fold and fault system that deformed the Valle Fértil Complex during Lower Palaeozoic times, and a Tertiary fracture system responsible for the present morphology (Mirré 1976).

ANALYTICAL TECHNIQUES

Electron microprobe analyses of alka-

TABLE 1: Representative electron microprobe analyses of feldspars from La Aguadita Trachyte (sample LA12-2).

Sample/ Point	SiO$_2$	Al$_2$O$_3$	FeO	Na$_2$O	K$_2$O	CaO	BaO	SrO	Total	Si	Al	Fe(ii)	Ca	Na	K	TOTAL	An	Ab	Or
LA 12-2 Feldspar 1	66.7	18.3	0.4	8.3	5.2	0.0	0.1	0.0	99.0	12.0	3.9	0.1	0.0	2.9	1.2	20.1	0.1	70.8	29.1
LA 12-2 Feldspar 2	66.3	18.1	0.3	6.6	7.4	0.0	0.0	0.0	98.7	12.1	3.9	0.0	0.0	2.3	1.7	20.0	0.1	57.3	42.6
LA 12-2 Feldspar 3	66.6	18.5	0.3	8.8	4.2	0.0	0.0	0.0	98.5	12.0	3.9	0.0	0.0	3.1	1.0	20.0	0.2	75.9	23.9
LA 12-2 Feldspar 4	66.7	18.6	0.3	9.7	2.9	0.0	0.1	0.0	98.4	12.0	3.9	0.0	0.0	3.4	0.7	20.1	0.2	83.3	16.5
LA 12-2 Feldspar 5	66.6	18.3	0.3	8.7	4.0	0.1	0.0	0.0	98.1	12.0	3.9	0.0	0.0	3.1	0.9	20.0	0.4	76.3	23.3
LA 12-2 Feldspar 6	66.4	18.3	0.3	6.0	8.0	0.0	0.0	0.0	99.1	12.1	3.9	0.1	0.0	2.1	1.9	20.0	0.1	53.0	46.9
LA 12-2 Feldspar 7	67.2	18.7	0.2	8.8	4.2	0.0	0.0	0.0	99.2	12.0	4.0	0.0	0.0	3.1	0.9	20.0	0.2	76.2	23.6
LA12-2 Kfs1	66.0	18.7	0.3	7.8	4.9	0.1	0.0	0.0	97.9	12.0	4.0	0.0	0.0	2.7	1.1	20.0	0.7	70.0	29.3
LA12-2 Kfs2	65.0	18.2	0.2	4.8	9.2	0.1	0.1	0.0	97.5	12.0	4.0	0.0	0.0	1.7	2.2	19.9	0.3	44.2	55.5
LA12-2 Kfs3	66.4	18.5	0.2	8.8	3.8	0.2	0.0	0.1	98.0	12.0	3.9	0.0	0.0	3.1	0.9	20.0	1.0	77.0	22.0
LA12-2 Kfs4	66.4	18.4	0.3	8.1	4.8	0.0	0.0	0.0	98.1	12.0	3.9	0.0	0.0	2.8	1.1	20.0	0.2	71.7	28.1
LA12-2 Kfs5	64.9	18.0	0.2	4.8	9.4	0.0	0.0	0.0	97.4	12.0	3.9	0.0	0.0	1.7	2.2	20.0	0.2	43.3	56.5
LA12-2 Kfs6	66.6	18.8	0.1	8.8	3.6	0.2	-0.1	0.0	98.0	12.0	4.0	0.0	0.0	3.1	0.8	19.9	1.0	78.0	21.0
LA12-2 Kfs7	66.6	18.6	0.1	7.2	5.7	0.1	0.0	0.0	98.3	12.0	4.0	0.0	0.0	2.5	1.3	19.9	0.6	65.4	34.0
LA12-2 Kfs8	65.2	18.3	0.3	5.3	8.7	0.0	0.1	0.0	97.9	12.0	4.0	0.0	0.0	1.9	2.1	20.0	0.2	47.7	52.1
LA12-2 Kfs9	66.8	18.3	0.1	8.0	4.5	0.1	0.1	0.0	98.0	12.1	3.9	0.0	0.0	2.8	1.0	19.9	0.6	72.6	26.8
LA12-2 Kfs11	66.7	18.1	0.6	7.2	5.5	0.0	0.0	0.3	98.5	12.1	3.9	0.1	0.0	2.5	1.3	19.9	0.2	66.1	33.6
LA12-2 Kfs12	64.8	16.4	2.7	6.8	4.5	-0.1	0.0	0.2	95.7	12.2	3.6	0.4	0.0	2.5	1.1	19.8	0.0	69.6	30.4
LA12-2 Kfs14	68.9	18.7	0.7	9.2	4.2	0.1	0.1	0.0	102.0	12.0	3.8	0.1	0.0	3.1	0.9	20.1	0.6	76.6	22.8
LA12-2 Kfs15	67.7	18.9	0.6	8.3	4.1	0.0	0.0	0.2	99.8	12.0	4.0	0.1	0.0	2.9	0.9	19.9	0.0	75.5	24.5
LA12-2 Kfs16	66.7	18.7	0.2	8.6	4.0	0.1	0.0	0.0	98.4	12.0	4.0	0.0	0.0	3.0	0.9	20.0	0.3	76.0	23.7
LA12-2 Kfs17	65.7	18.3	0.2	5.8	8.1	0.1	0.1	0.0	98.3	12.0	4.0	0.0	0.0	2.0	1.9	20.0	0.2	51.7	48.1
LA12-2 Kfs18	66.7	18.5	0.4	8.9	3.8	0.0	0.0	0.0	98.4	12.0	3.9	0.1	0.0	3.1	0.9	20.0	0.2	78.0	21.8
LA12-2 Kfs19	66.0	18.2	0.2	6.5	6.7	0.0	0.0	0.0	97.8	12.1	3.9	0.0	0.0	2.3	1.6	19.9	0.1	59.3	40.5

* Cations based on 32 oxygens, end members in %. Oxides in wt.%, total iron as FeO.

li feldspar and amphibole on a selected sample of trachyte (sample LA12-2) (Tables 1-2), were carried out using a JEOL JXA-8230 SuperProbe electron microprobe equipped with two wavelength dispersive X-ray spectrometers (WDS) and an energy dispersive X-ray spectrometer (EDS), hosted at LAMARX (Laboratorio de Microscopía Electrónica y Análisis por Rayos X), University of Córdoba, Argentina. Microprobe running conditions were 15.0 kV high voltage, 20 nA beam current and 3 μm electron beam. Detection limits were approximately 0.03 % for light elements (expressed as oxides) and 0.08 % for heavy elements (expressed as oxides). Standard materials used in alkali feldspar determination were: anorthoclase (Na, Al, Si), benitoite (Ba), fayalite (Fe$_2$O$_3$), orthoclase (K), wollastonite (Ca) and celestine (Sr). Standard reference materials for amphibole were: topaz (F), anorthoclase (Na, Al), diopside (Mg, Si, Ca), fayalite (FeO), orthoclase (K), sphene (Ti), Bushveld chromite (Cr), sodalite (Cl) and rodonite (Mn). Ferrous and ferric Fe were calculated using the equation of Droop (1987). Data processing was made using the Excel spreadsheets GabbroSoft 2013 (http://www.gabbrosoft.org/spreadsheets.html).

Twenty seven representative fresh samples of mafic and felsic volcanic rocks from Sierra de Valle Fértil -amongst which four samples belong to La Aguadita Trachyte-, were selected and analysed for whole rock geochemistry. Major and minor oxides were determined on fused lithium borate glass pellets by X-ray fluorescence spectrometry (XRF), and trace elements and rare earth element (REE) contents were determined by inductively coupled plasma-mass spectrometry (ICP-MS) at ALS Minerals Laboratories, Canada. Analytical precision is 0.01 % for major element oxides Al$_2$O$_3$, CaO, Fe$_2$O$_3$, MgO and SiO$_2$, and 0.001 % for BaO, Cr$_2$O$_3$, K$_2$O, MnO, Na$_2$O, P$_2$O$_5$ and SrO. For trace elements and REE precision is 5 ppm (V), 2 ppm (Mo, Zr), 1 ppm (W), 0.5 ppm (Ba, Ce, Co, La, Tl, Y), 0.2 ppm (Hf, Nb, Rb), 0.1 ppm (Ga, Nd, Sr, Ta), 0.05 ppm (Dy, Gd, Th, U), 0.03 ppm (Er, Eu, Pr, Sm, Yb) and 0.01 ppm (Cs, Ho, Lu, Tb, Tm). Whole rock and REE analyses for the trachyte samples are given in table 3.

The K/Ar dating on a selected sample of the La Aguadita Trachyte (sample LA12-2) was performed in the Laboratory of Geochronology, Servicio Nacional de Geología y Minería (SERNAGEOMIN), Chile. Sample was degassed by high-frequency induction heating. The argon was cleaned and purified in Pyrex extraction lines and the radiogenic ^{40}Ar volumes were determined using isotopic dilution techniques in an MS10S Mass Spectrometer, with a total accuracy of 1-2%. The K analyses were done in triplicate by atomic absorption techniques with an accuracy of 0.7-1.3%, depending on the K content and using a Li-internal standard. The interlaboratory standard GL-0 was used for controlling and for the calibration of Ar and K determination. Errors in K-Ar ages are quoted at the two sigma (2σ) level and the decay constants are those suggest-
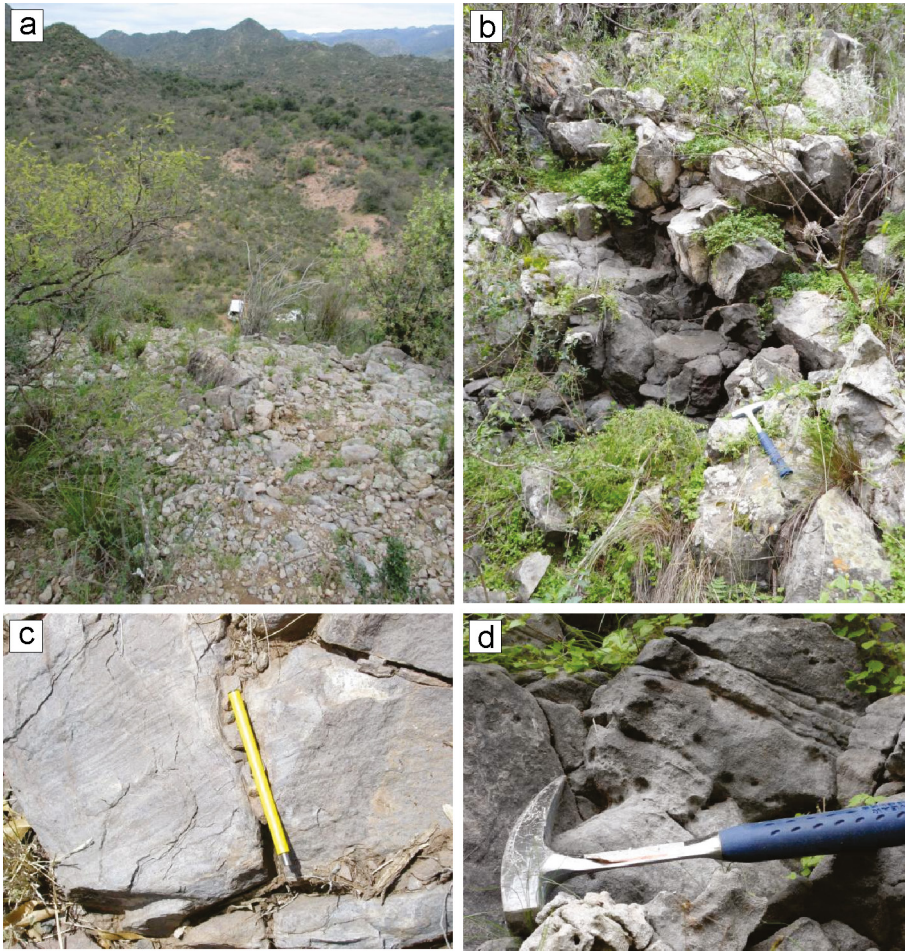
Figure 2: a) View from the top of the trachyte outcrop to the west showing the main body of Sierra de Valle Fértil at the bottom; b) Massive trachyte outcrop; c) Flow-banded structure; d) Vesicles in the upper section of the trachyte body.

ed by Steiger and Jager (1977). These include an estimated error for the standards and an error for the Ar isotope ratios. Data are reported in table 4. Rb/Sr and Sm/Nd isotope ratios from a representative sample (sample LA7) were obtained by whole rock isotope dilution technique at the Centro de Pesquisas Geocronologicas (CPGeo), Universidade de Sao Paulo, Brazil. Data and procedures for the analysis are specified in tables 5 and 6.

LA AGUADITA TRACHYTE: FIELD OCCURRENCE AND PETROGRAPHY

La Aguadita Trachyte lies on the eastern side of the Río del Potrero graben (30°46'24.26" S - 67°26'16.02" W), along the main NNW-trending Portezuelo Lineament (Furque *et al*. 1999) that sep-

arates the main body of Sierra de Valle Fértil from its eastern portion (Fig. 1b). Uplift and strong erosion have resulted in incomplete exposure of this lithology, supposed to be a remnant of a lava dome. La Aguadita Trachyte consists of a 15 - 20 m thick whitish-grey microporphyritic to aphanitic lava body that overlies metatonalites, granodiorites and granites of the crystalline basement covering an area of approximately 120 m × 200 m (Figs. 2a-b). Outcrops of Los Molles - Los Bretes Basaltic Trachyandesite (López 2011) are also exposed in the surroundings; however, no contact relationships are seen between them.

The trachytic rock exhibits a distinct but thinly flow structure in the field (Fig. 2c), clearly observed on weathered surfaces of the outcrop with the appearance of light grey and ochre colour bands or

streaks. Moreover, small ellipsoidal and rounded vesicles up to 0.7 cm in diameter are occasionally seen in the upper part of the body (Fig. 2d).

The trachyte consists of alkali feldspar ± sodium-rich amphibole. Iron oxides (magnetite and hematite), and tiny zircon grains with pleochroic halos included in the feldspars, are the main accessories. The feldspar, ranging from sanidine to anorthoclase, is completely dominant (≈ 90 % total volume). It is present both as twinned and zoned euhedral phenocrysts and microphenocrysts (up to 1 mm in size) as in the orthophyric to slightly trachytic groundmass (0.07 - 0.6 mm in size), (Figs. 3a-b). Feldspar crystals have micro- to cryptoperthitic textures, anomalous extinction, and show polysynthetic or combined Carlsbad-polysynthetic twinning (Figs. 3c-e). Feldspars are generally fresh or slightly altered to kaolinite. Most feldspar phenocrysts are oscillatory zoned (Figs. 4a-c), revealing regular variations in the Or molecule between cores and rims as seen in figure 4b, where the feldspar crystal shows a core of Ab_{72} mantled by $Ab_{45.5}$ and again by Ab_{72} in the outer zone of the crystal. Na content in feldspars varies from Ab 43 to 83 % averaging about $An_{0.32}$-$Ab_{67.33}$-$Or_{32.35}$ (Table 1). On the ternary Ab-An-Or diagram of Deer *et al*. (1966), the feldspars display a compositional array from sodic sanidine to anorthoclase (Fig. 4d, Table 1). The average mineral formula is $Na_{0.66}K_{0.32}Fe^{2+}_{0.01}Al_{0.98}$ $Si_{3.01}O_8$.

Subsidiary deep-blue sodium-rich amphibole, zoned and strongly pleochroic in shades of deep blue, indigo to yellow-brown, is present as interstitial crystals in the groundmass. The fine-grained alkali amphibole is recorded as rare groundmasses phase in trachyte elsewhere (Nono *et al.* 1994). The amphibole occurs as small (< 0.09 mm) anhedral to subhedral crystals and as spongy aggregates, filling the interstices between the feldspars (Fig. 3f). It is often rimmed by iron oxides. All the analysed amphibole crystals occurring in the trachyte are of sodic amphibole in the sense of Leake *et al.* (1997), where $Na_B \geq$ 1.5 and $(Na+K)_A \geq 0.5$. They have a max-

imum $Mg/(Mg+Fe^{2+})$ ratio of 0.0029 indicating Fe-rich types (Table 2). The high fluorine content ($\approx$ 2.33 wt.% in average) should be emphasized. According to the amphibole nomenclature of Leake *et al.* (2003), the composition fluctuates between arfvedsonite to ferro-eckermannite (Fig. 4f). Compositional variations of feldspar and amphibole are shown in figures 4d and 4f, respectively.

Even though La Aguadita Trachyte contains nearly 70 wt.% SiO_2 and up to 10.7 % normative quartz, modal quartz is absent or rarely seen and confined to the groundmass.

GEOCHEMISTRY

The trachyte has SiO_2 content which ranges from 66.5 % to 69.1 and exhibits a limited compositional range in most of the major elements: 15.5 - 16.1 % Al_2O_3, 2.56 - 2.76 % Fe_2O_3, 0.03 - 0.09 % MgO, < 0.01 - 0.02 % TiO_2, 0.01 - 0.14 % P_2O_5, 0.36 - 1.22 % CaO, 7.2 - 7.35 % Na_2O and 4.3 - 4.5 % K_2O (Table 3). The average alkali content is of 11.7 %, with average Na_2O content of 7.27 %. In contrast, the trachyte shows a wide compositional range in Zr (982 - 1580 ppm) and Sr (7 - 82.5 ppm). On the total alkalis *vs.* silica diagram (after Le Maitre 1989, Fig. 5a), the trachyte lies within the alkaline field. Consistently, its composition occurs on the comenditic trachyte field of the binary Nb/Y-SiO_2 diagram (after Winchester and Floyd 1977, Fig. 5b). The trachyte samples have significant amount of normative quartz (6.5 to 10.7 wt.%) and also have acmite (up to 4.4 wt.%) in the norm. La Aguadita Trachyte displays remarkable Zr enrichment when compared with other incompatible trace elements (e.g. Zr/Rb = 5.73, Zr/Th = 22.72, Zr/La = 10.64 and Zr/Ce = 5.45, in average). On the primitive mantle normalized trace element plot (Fig. 6a) using normalization values of Sun and McDonough (1989), the La Aguadita Trachyte shows significant negative anomalies in Ba, Sr, P and Ti, which indicates plagioclase, apatite and Fe-Ti oxide fractionation. Low concentrations for Ba ($\leq$ 28.8 ppm) are al-
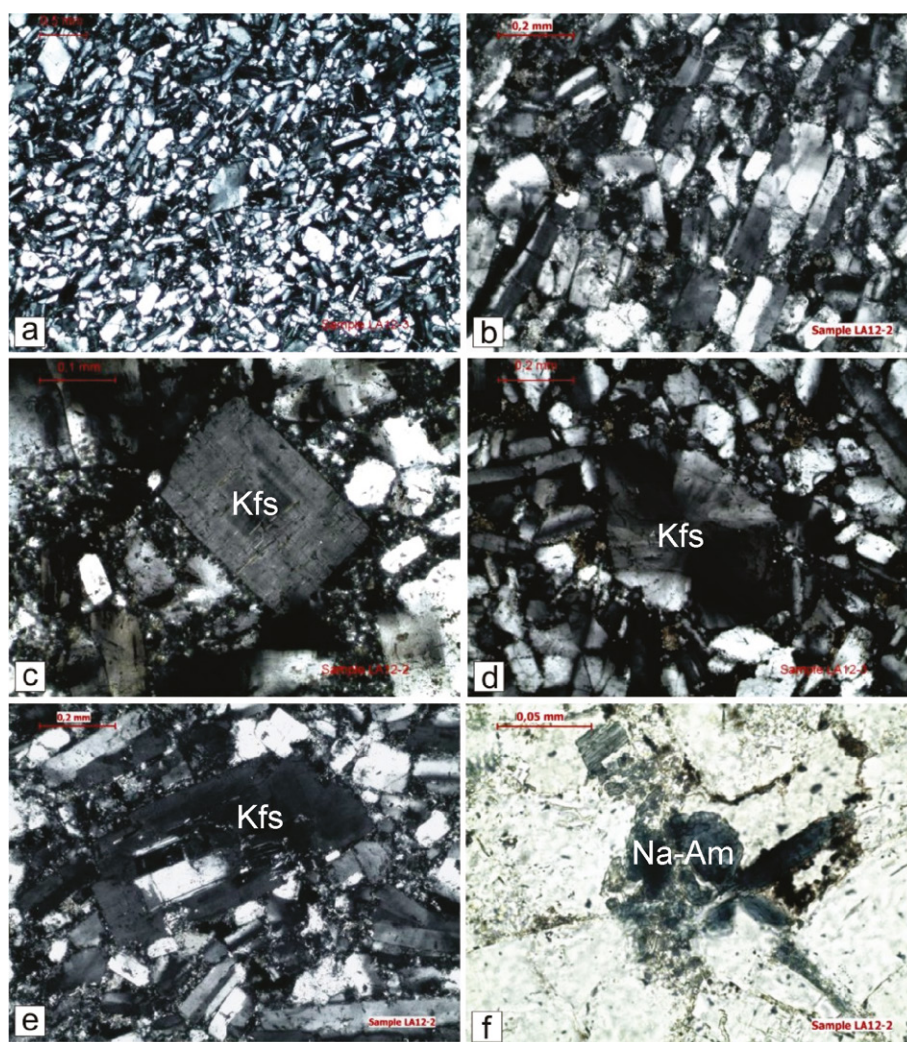

Figure 3: Photomicrographs of La Aguadita Trachyte: a) Orthophyric groundmass characterized by closely packed feldspar crystals with quadratic or short and stumpy rectangular cross sections (NX); b) Trachytic texture due to the alignment of feldspar laths (NX); c) Euhedral anorthoclase microphenocryst exhibiting zoning and tartan twinning; d) Zoning and anomalous extinction in anorthoclase microphenocryst (NX); e) Normal-zoned feldspar microphenocryst (NX); f) Zoned and strongly pleochroic alkali amphibole crystals (N//). N//: plane polarized light; NX: crossed polarized light. Mineral abbreviations after Siivola and Schmid (2007).

so attributed to alkali feldspar fractionation. On the other hand, Rb reaches levels of 193-259 ppm equal to 400 times primitive mantle levels, Zr is at up 1580 ppm (1235 ppm average) and Nb is at up 231 ppm (207 ppm average) with Zr/Nb = 5.97. The abundance of high field strength elements (HFSE) such as Y, Yb, Lu (20-40 times primitive mantle values), is also remarkable.

The chondrite-normalized REE pattern of the La Aguadita Trachyte (chondrite values after Nakamura 1974) has steep light rare earth elements (LREE) and almost flat heavy rare earth elements

(HREE) profile (Fig. 6b). The REE pattern is enriched in LREE [$(La/Sm)_N$ = 5.08] relative to HREE [$(Gd/Lu)_N$ = 0.93] and shows a fractionated ratio between $(La/Yb)_N$ = 5.64, with negative Eu anomaly (Eu/Eu* $\approx$ 0.185 on average).

K-AR AGE DATING AND ISOTOPY

The radiometric age of 218 ± 7 Ma obtained by the K/Ar method on whole rock (Table 4) provides evidence that igneous activity, which is related to extensional tectonics and could have begun in

TABLE 2: Representative electron microprobe analyses of amphiboles from La Aguadita Trachyte (sample LA12-2).*

Sample/Point	SiO_2	TiO_2	Cr_2O_3	Al_2O_3	FeO	MnO	MgO	CaO	ZnO	Na_2O	K_2O	Cl	F	Total
LA 12-2Amp1-12	50.59	0.19	0.02	0.25	31.61	1.76	0.04	0.30	0.28	8.85	1.29	0.00	3.12	96.99
LA 12-2Amp2-12	50.52	0.17	-0.01	0.20	31.28	1.91	0.00	0.27	0.28	8.35	1.35	0.00	3.12	96.13
LA 12-2Amp3-12	50.02	0.13	-0.04	0.25	31.52	1.83	0.01	0.31	0.28	8.12	1.45	0.02	3.13	95.69
LA 12-2Amp4-12	50.15	0.14	-0.01	0.21	0.21	1.83	0.00	0.21	0.23	8.32	1.43	0.01	3.12	95.44
LA 12-2Amp1	52.04	0.12		0.27	30.83	1.66	0.03	0.32	0.15	9.97	1.32	0.00	1.58	98.29
LA 12-2Amp2	51.08	0.16		0.29	30.82	1.63	0.03	0.30	0.20	9.87	1.25	0.02	1.39	97.02
LA 12-2Amp4	51.68	0.23		0.26	30.73	1.58	0.02	0.38	0.27	9.75	1.39	0.03	1.53	97.84
LA 12-2Amp5	51.71	0.14		0.26	30.52	1.48	0.01	0.26	0.21	9.83	1.33	0.00	1.65	97.38

Sample/Point	Si	Al(IV)	Al(VI)	Fe^{3+}	Ti	Cr	Fe^{2+}	Mn	Mg	Ca	Na	K	Total	$Mg/(Mg+Fe^{2+})$
LA 12-2Amp1-12	8.25	-0.25	0.29	0.47	0.02	0.00	3.83	0.24	0.01	0.05	2.80	0.27	16.00	0.0029
LA 12-2Amp2-12	8.35	-0.35	0.38	0.19	0.02	0.00	4.14	0.27	0.00	0.05	2.67	0.28	16.00	0.0000
LA 12-2Amp3-12	8.32	-0.32	0.37	0.21	0.02	0.00	4.17	0.26	0.00	0.06	2.62	0.31	16.00	0.0002
LA 12-2Amp4-12	8.34	-0.34	0.38	0.23	0.02	0.00	4.10	0.26	0.00	0.04	2.68	0.30	16.00	0.0001
LA 12-2Amp1	8.24	-0.24	0.29	0.77	0.01	0.00	3.31	0.22	0.01	0.05	3.06	0.27	16.00	0.0018
LA 12-2Amp2	8.19	-0.19	0.25	0.84	0.02	0.00	3.29	0.22	0.01	0.05	3.07	0.25	16.00	0.0021
LA 12-2Amp4	8.24	-0.24	0.29	0.70	0.03	0.00	3.40	0.21	0.01	0.06	3.01	0.28	16.00	0.0018
LA 12-2Amp5	8.28	-0.28	0.33	0.68	0.02	0.00	3.41	0.20	0.00	0.05	3.05	0.27	16.00	0.0006

* Calculations assuming 16 cations and no A - site vacancies. Oxides in wt.%, total iron as FeO.

TABLE 3: Whole rock chemical composition and some geochemical parameters of La Aguadita Trachyte.

SAMPLE	SiO_2	Al_2O_3	Fe_2O_3	CaO	MgO	Na_2O	K_2O	TiO_2	MnO	P_2O_5	LOI	Total
LA7	66.6	15.95	2.70	0.47	0.09	7.35	4.48	<0.01	0.11	0.02	0.44	98.3
LA12-2	66.5	15.75	2.56	1.22	0.08	7.21	4.44	0.02	0.09	0.01	1.05	98.9
LA12-3	66.8	16.10	2.70	0.84	0.03	7.30	4.42	0.02	0.07	0.07	0.73	99.1
LA12-4	69.1	15.50	2.76	0.36	0.09	7.22	4.35	0.02	0.11	0.14	0.53	100

SAMPLE	Ba	Ce	Co	Cr	Cs	Dy	Er	Eu	Ga	Gd	Hf
LA7	22.0	207	0.7	50	0.28	14.30	9.88	0.63	56.7	11.90	32.4
LA12-2	28.8	196	0.8	<10	0.15	16.95	11.60	0.88	55.7	13.95	32.8
LA12-3	22.0	243	0.6	<10	0.14	25.80	18.10	1.22	57.1	21.30	47.7
LA12-4	26.7	248	0.7	50	0.22	21.00	14.05	1.06	58.3	16.90	46.1

SAMPLE	Ho	La	Lu	Mo	Nb	Nd	Pr	Rb	Sm	Sn	Sr
LA7	2.99	105	1.63	3	211	65.4	19.7	259	12.95	29	7.0
LA12-2	3.66	88	1.79	<2	202	63.6	18.7	228	12.90	32	11.4
LA12-3	5.49	110	2.87	<2	231	80.0	23.7	208	18.65	31	11.4
LA12-4	4.32	181	2.11	<2	185	77.0	26.9	193	14.95	39	82.5

SAMPLE	Ta	Tb	Th	Tl	Tm	U	V	W	Y	Yb	Zr
LA7	30.0	2.01	54.5	<0.5	1.67	6.63	22	3	100	12.20	982
LA12-2	31.5	2.47	49.7	<0.5	1.83	7.51	7	2	116	12.40	998
LA12-3	30.2	3.77	50.2	<0.5	2.81	11.1	11	2	182	18.85	1580
LA12-4	41.9	2.96	64.4	<0.5	2.19	5.22	10	2	138.5	14.85	1380

SAMPLE	Eu*	Eu/Eu*	(Gd/Lu)N	(La/Lu)N	(La/Sm)N	Ce/U	(La/Yb)N	Nb/La	Nb/U	Nb/Y	Th/Nb
LA7	4.06	0.15	0.89	6.64	5.00	31.22	5.75	2.01	31.82	2.11	0.26
LA12-2	4.39	0.20	0.96	5.06	4.21	26.10	4.75	2.29	26.89	1.74	0.25
LA12-3	6.52	0.19	0.91	3.95	3.64	21.90	3.90	2.10	20.81	1.27	0.22
LA12-4	5.20	0.20	0.98	8.84	7.47	47.50	8.15	1.02	35.44	1.33	0.35

SAMPLE	Y/Nb	Zr/Ce	Zr/La	Zr/Nb	Zr/Rb	Zr/Th	La/Yb
LA7	0.47	4.7	9.35	4.65	3.80	18.0	8.61
LA12-2	0.57	5.1	11.3	4.94	4.37	20.0	7.10
LA12-3	0.79	6.5	14.3	6.84	7.60	31.5	5.83
LA12-4	0.75	5.5	7.60	7.46	7.15	21.4	12.19

Major oxides in wt.%, trace elements and rare earth elements in ppm, total iron as Fe_2O_3. LOI: loss on ignition.

the Lower Triassic (Page *et al.* 1997), certainly continued until at least the uppermost Triassic.

Initial ($^{87}Sr/^{86}Sr$)0 ratios were calculated for an age of 218 Ma and also for the extreme values from the error interval 211 - 225 Ma (Table 5). An anomalous low Sr_0 isotopic ratio was obtained (Sr_0 = 0.65993). Because alteration observed in La Aguadita Trachyte is insignificant, the most probable explanation for the anomalously low calculated initial value would be in relation to the very low Sr content (5.5 ppm). Due this very low Sr content, small variations produced by slightly alteration could produce perturbation on the Rb-Sr system during or after trachyte emplacement. A similar explanation was proposed by Dahlquist *et al.* (2010) in Carboniferous A-type granitoids from Sierras Pampeanas. These authors indicate that anomalous samples also show lower Sr contents, probably reflecting perturbation of the Rb-Sr systematics after crystallization by an alteration event. In our case, originally samples would have very low Sr contents, and under this condition slightly modifications of Rb-Sr contents for incipient alteration could affect the ($^{87}Sr/^{86}Sr$) ratio.

Sm-Nd isotopes are quoted in Table 6. ($^{143}Nd/^{144}Nd$)0 calculated for an age of 218 Ma yields a value of 0.512357, with an εNd = +2.6, εNd_{CHUR} = 0.3 and a TDM of 0.65 Ga. Positive but relatively low εNd values (+2.6) suggest a parental mantle-derived magma that could incorporate some crustal component during its ascent throughout continental crust (Nohda and Wasserburg 1981, Davidson 1987).

DISCUSSION

The tectonic setting of La Aguadita Trachyte is considered by taking into account its geochemistry in order to understand its geological history and the nature of any genetic process during its evolution. The largest volumes of peralkaline silicic rocks are found in areas of rift formation on the continents, but they may also form in several other tectonic settings such as in areas of extensional tec-
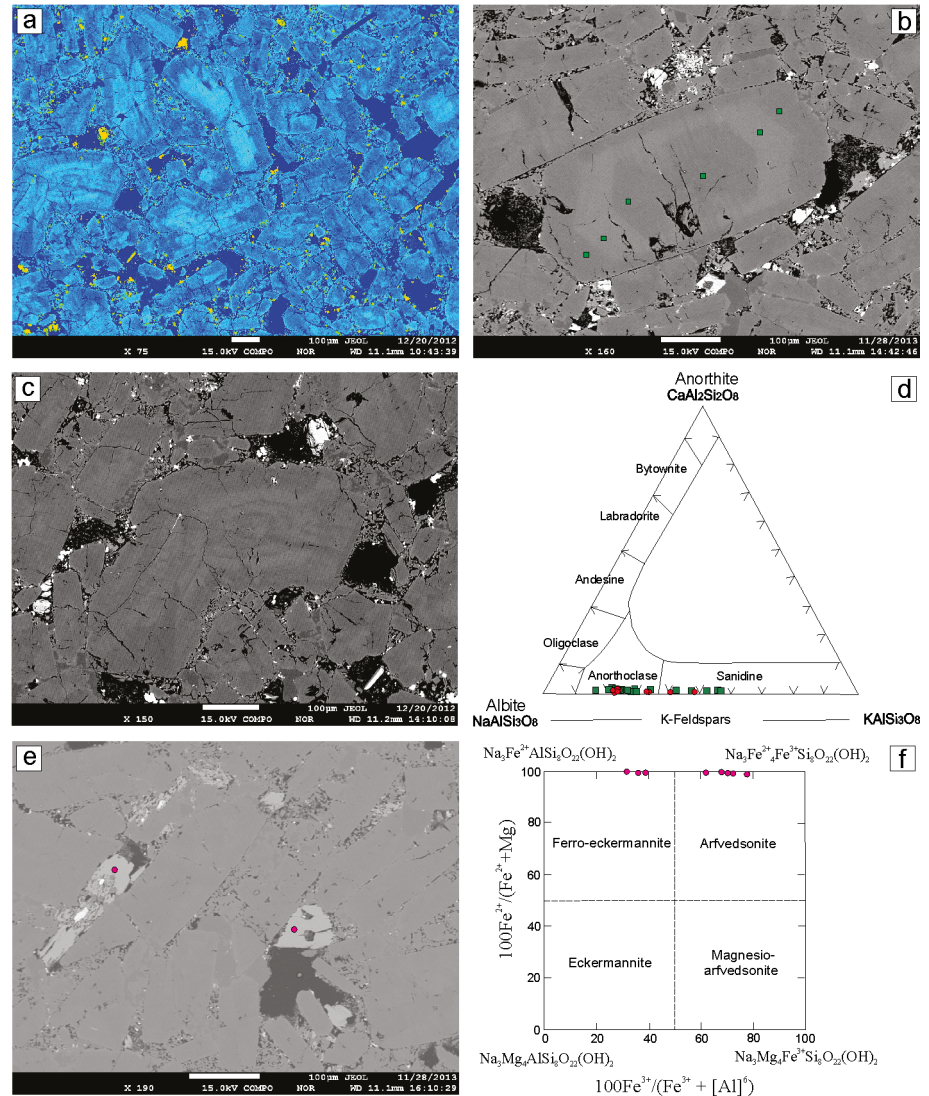
Figure 4: La Aguadita Trachyte, sample LA12-2: a) False-color backscattered electron (BSE) image showing the orthophyric texture and strong zoning in anorthoclase crystals; b) BSE image of alkali feldspar microphenocryst showing the position of the EDS analysed points; c) BSE image of zoned anorthoclase crystals; d) Chemical classification of feldspars in the Ab-An-Or diagram (after Deer *et al.* 1966). Filled squares: phenocrysts/microphenocrysts, filled circles: groundmass feldspars; e) BSE image of interstitial amphibole (dots); f) Classification diagram of amphiboles (dots) from La Aguadita Trachyte (after Leake *et al.* 2003).

tonics (MacDonald 1974b). The peralkaline character of La Aguadita Trachyte is supported by the presence of arfvedsonite and ferro-eckermannite as minor phase. Furthermore, in the FeO_T (total iron) *vs.* Al_2O_3 diagram (MacDonald 1974a, Fig. 6c), the studied trachyte samples are grouped together in the field of the peralkaline trachytes (comenditic trachytes) which are typical of continental rift-valley systems. The Rb, U, Th, Nb, Ta, Y, Zr, and REE contents are relatively abundant suggesting geochem-

ical features of intraplate magmatism (White and Urbanczyk 2001). Enrichment in alkalis, as well as in LREE relative to HREE [$(La/Yb)_N$ = 5.64 chondrite normalized according to Nakamura 1974], are features of intraplate alkaline magmas worldwide. In the appropriate discrimination diagrams (Figs. 6d-e) the geochemistry of La Aguadita Trachyte is consistent with a continental rift setting. The high Nb contents are also typical of intraplate magmas (Wilson 1989). The tectonic setting is corroborated by the
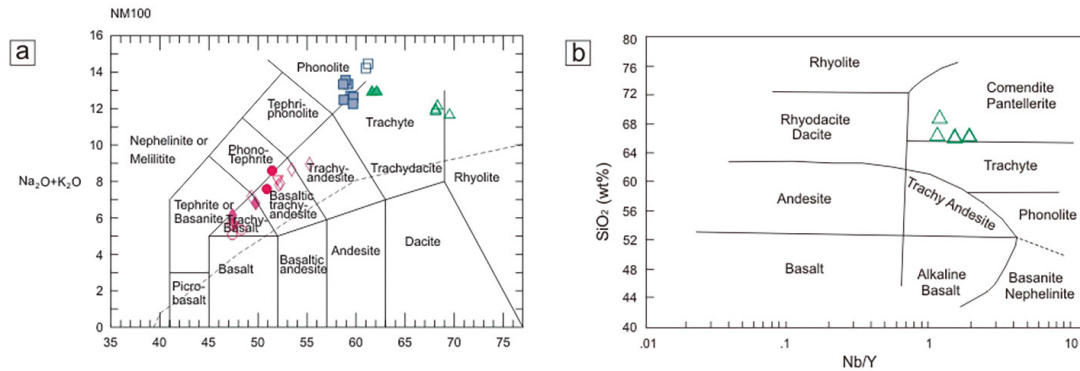
Figure 5: a) Total alkali *vs.* SiO$_2$ diagram for the entire analysed alkaline rocks of Sierra de Valle Fértil (after Le Maitre 1989, normalized to 100%, water free). The line after Irvine and Baragar (1971) illustrates the alkaline nature of the rocks; b) Nb/Y-SiO$_2$ diagram (after Winchester and Floyd 1977). Oxide contents in wt.%; trace elements in ppm. Symbols: filled rhombus: San Agustín Basalt, open circle: Potrerillos Basalt, filled circle: Usno Basalt, unfilled inverted triangle: Tala - Turbante Basalt, unfilled rhombus: Los Molles - Los Bretes Basaltic Trachyandesite, unfilled square: Jaboncillo Trachyphonolite Phonolite, filled square: Monte Chumao Phonolite, filled triangle: Loma Negra Trachyte, unfilled triangle: La Aguadita Trachyte.
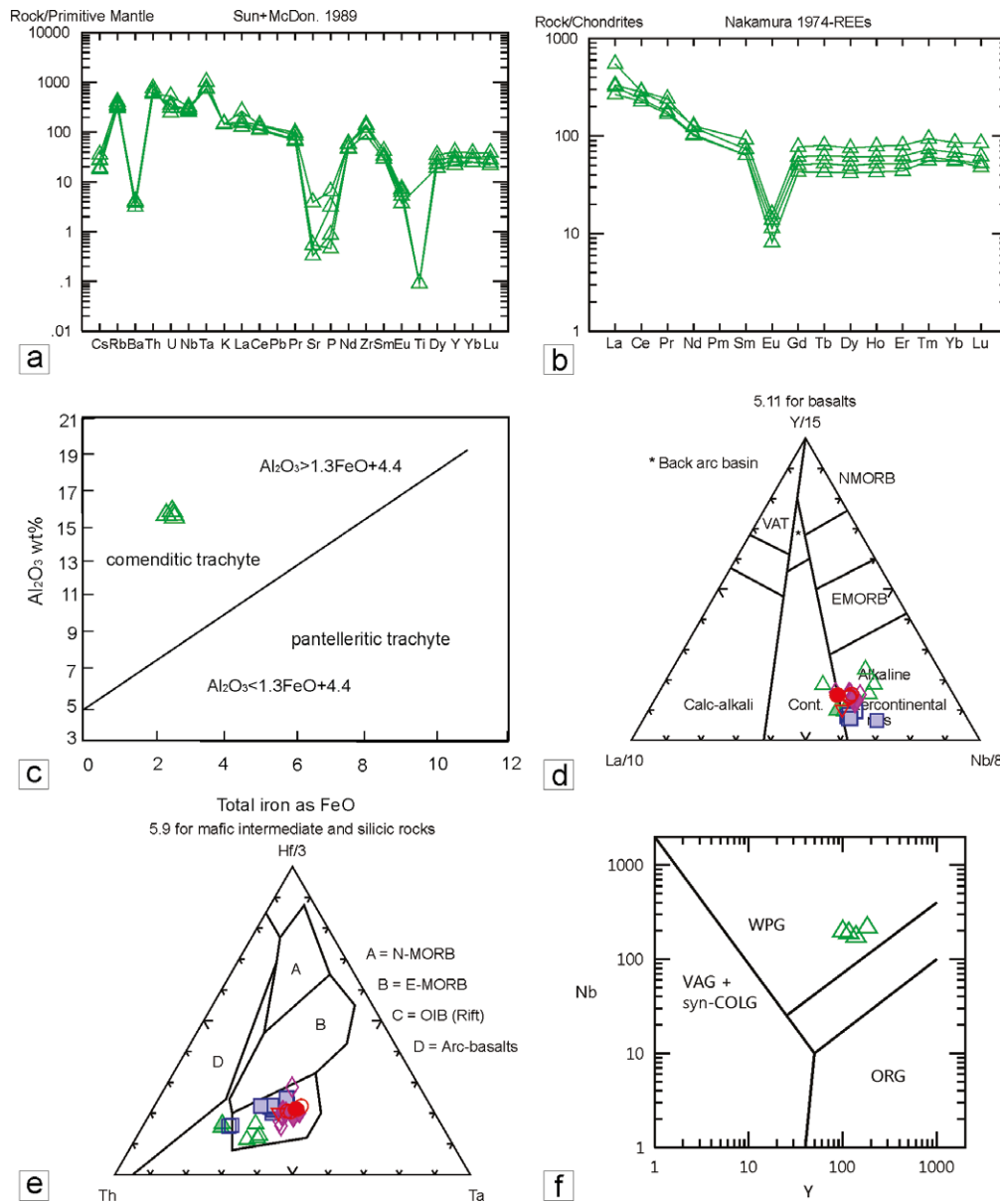
Figure 6: a) Primitive mantle-normalized incompatible trace element pattern for La Aguadita Trachyte (normalization values after Sun and McDonough 1989); b) Chondrite-normalized REE pattern for La Aguadita Trachyte (normalization values after Nakamura 1974); c) In the Al$_2$O$_3$ *vs.* FeO$_{total}$ diagram (after Macdonald 1974 modified by Kozlovsky *et al.* 2007) the analysed trachyte samples are grouped into the comenditic field; d-e) La/10-Y/15-Nb/8 (Cabanis and Lecolle 1989) and Th-Hf/3-Ta (Wood 1980) discrimination diagrams showing that the entire alkaline rocks from Sierra de Valle Fértil -including La Aguadita Trachyte-, plot in the within-plate setting; f) Y *vs.* Nb tectonic discriminant diagram of Pearce *et al.* (1984). WPG: within-plate granites, COLG: collisional granites, VAG: volcanic arc granites, ORG: ocean-ridge granites. Oxide contents in wt.%; trace elements and REE in ppm. Symbols as in Fig. 5.

Nb-Y ratios, plotting the analysed trachyte in the within-plate granitoids domain defined by Pearce *et al.* (1984) (Fig. 6f).

As with most continental alkaline rocks, the whole volcanic rocks from Sierra de Valle Fértil are associated with extensional block faulting resulting from distant and/or local stress fields related to the Triassic rifting, and were emplaced along lines of lithospheric weakness. Rift-triggered magmatism with Middle- to Upper Triassic ages ranging from 231 to 215 Ma is common in the Ischigualasto-Villa Union basin. Moreover, extensional fault-controlled A-type granitoids have been also defined by Dahlquist *et al.* (2010) during Carboniferous time in the Eastern Sierras Pampeanas, indicating that this relation between alkaline acid magmatism and extensional setting is recurrent in the time and evolution of the region.

In general, and as proposed by Gharib *et al.* (2012 and references therein), the various sources of trachytic rocks are summarized as follows: (1) fractional crystallization of mantle-derived magma source, either during major lithospheric extension or when a mantle plume impinges the base of the lithosphere; (2) interaction of mantle-derived magmas with continental crustal materials to produce trachytic melts; and (3) mixing of independent mafic and felsic magmas.

Field, petrographic and geochemical characteristics of the La Aguadita Trachyte such as the absence of any acidic or basic microgranular xenoliths, its homogeneous petrography, and the limited major and trace element variations, contradicts the magma mixing model as the process responsible for the magmatic evolution. Thus, the two remaining possible sources are (1) and (2). Moreover, most of feldspar phenocrysts are oscillatory zoned clearly indicating the changing chemical environment the crystals were subjected to during crystallization. Many alkaline rocks representing fractionates of dominant mantle-derived magma are characterized by low Y/Nb ratios (O'Halloran 1985) and low initial $^{87}Sr/^{86}Sr$ values (≈ 0.704; Faure and Pow-

TABLE 4: K/Ar age dating on La Aguadita Trachyte.

Sample identification	Material	% K	Rad. Ar nl/g	Atmospheric Ar %	Age Ma	Error (2σ)
LA12-2	Whole -rock	3.780	34.009	3	218	±7

TABLE 5: Rb-Sr isotope analyses of La Aguadita Trachyte.

Sample	Material	Rb	Sr	$^{87}Rb/^{86}Sr$	$^{87}Sr/^{86}Sr$	Error (2σ)	$(^{87}Sr/^{86}Sr)_0$
LA7$_{218}$	RTOT/Trachyte	261.0	5.5	137.26	1.085501	0.000060	0.65993
LA7$_{225}$							0.64625
LA7$_{211}$							0.67362

* Initial $(^{87}Sr/^{86}Sr)_0$ ratios were calculated for a crystallisation age of 218 Ma and also for the extreme values given by the 2σ error of 225 and 211 Ma. $^{87}Sr/^{86}Sr$ ratio normalized to $^{86}Sr/^{88}Sr = 0.1194$.
Average $^{87}Sr/^{86}Sr$ ratio for the standard NBS-987 since January-October /2012 = 0.710244 ± 0.000036.
RTOT: whole-rock; Rb and Sr (in ppm) determined by XRF.

ell 1972) and consequent high εNd values. La Aguadita Trachyte displays fractionated REE pattern, and shows narrow variation range of Zr/Nb (4.65 - 7.46) and low Y/Nb ratio (< 0.8) close to oceanic island basalts (OIB) derived from mantle source. This variation range is due to the fact that Zr and Nb behave as very incompatible elements in alkaline magmas (Macdonald *et al.* 1987) (Fig. 7a). In addition, the positive but relatively low obtained εNd value of +2.6 would suggest a dominant primary mantellic source but with a slightly degree of crustal participation. This geochemical signature is also consistent with the projection in the Eby (1992) discriminant diagram proposed for distinguishing between mantle derived *vs* crustal-derived source in A-type magmatism. Relatively low Nb contents, compared with Y and Ga, plot our samples in the A1 group (Fig. 7b), suggesting a distinct mantle-source for La Aguadita Trachyte genesis.

The deep and nature of the mantle source are the dominant factors controlling the mantle-derived melts. According to Smith *et al.* (1999), HFS elements such as Nb are depleted in the lithospheric mantle relative to the LREE (such as La) with Nb/La ratios < 0.5. The high Nb/La ratio (≈ 1.85) and low La/Yb ratio (≈ 8.43) of La Aguadita Trachyte would suggest a depth mantle source.

The evolved geochemical signature of La Aguadita Trachyte, reflected by the negative Ba, Sr, and Eu anomalies, the low contents of CaO, Fe_2O_{3T}, MgO, TiO_2 and

P_2O_5 and the decrease in LREE from La to Sm, indicate that the trachyte has experienced a significant fractionation process. The Ba, Sr, Ti and P anomalies can be attributed to the fractionation of feldspars (Ba and Sr), titanomagnetite (Fe, Ti), and apatite (P). The negative Eu anomaly, together the very low-Sr content, reflect that Ca-rich plagioclases were major fractionation phases during the magmatic evolution. Dahlquist *et al.* (2010) find similar REE patterns for the Early Carboniferous A-type granites of Sierras Pampeanas. These authors conclude that progressive fractional crystallization with dominant fractionation of feldspar could explain the distinctive negative Eu anomalies observed in these A-type granites. Also, the gradual increase in Nb and Y contents with the increase of Zr content supports the fractional crystallization model of La Aguadita Trachyte. The high fluorine content (about 2.33 wt.%) in the alkali amphibole could reflects late-stage crystallization of volatile-rich alkaline liquids, or even an originally F enrichment in the parental magma as suggested by Dahlquist *et al.* (2010, 2014) for A-type granitoids.

The assimilation of crust by mantle derived melts is often invoked to explain the genesis of silica-oversaturated trachytic magmas (Panter *et al.* 1997 and references therein). Trace element Nb/U and Ce/U ratios in mafic and intermediate magmas are useful in distinguishing between mantle and crustal components and could help in the identification of

TABLE 6: Sm-Nd isotope analyses of La Aguadita Trachyte.

Sample	Sm	Nd	$^{147}Sm/^{144}Nd$	Error[1]	$^{143}Nd/^{144}Nd$	Error (2σ)	$(^{143}Nd/^{144}Nd)_0$	$\varepsilon Nd_{CHUR}{}^t$	εNd_{CHUR}	tDM (Ga)
LA7[218]	11.765	61.950	0.1148	0.0007	0.512655	0.000010	0.512491	2.6	0.3	0.65
LA7[225]							0.512486	2.7	0.3	0.65
LA7[211]							0.512496	2.5	0.3	0.65

* Initial $(^{143}Nd/^{144}Nd)_0$ ratios and $\varepsilon Nd_{CHUR}{}^t$ were calculated for a crystallisation age of 218 Ma and also for the extreme values given by the 2σ error of 225 and 211 Ma. $^{147}Sm/^{144}N$ ratios = [(ConcSm/ConcNd)*0.604491]. [1]Errors for the $^{147}Sm/^{144}Nd$ ratio and model age T_{DM} calculated from the spread of analytical errors in the variables used in the respective equations. $^{143}Nd/^{144}Nd$ ratios (measured as Nd$^+$) normalized to $^{146}Nd/^{144}Nd = 0.7219$ (De Paolo 1981). Model age $T_{DM} = 1/l^{147}Sm * ln \{[(^{143}Nd/^{144}Nd)_{am} - (^{143}Nd/^{144}Nd)_{DM}]/[(^{147}Sm/^{144}Nd)_{am} - (^{147}Sm/^{144}Nd)DM] + 1\}$. $\varepsilon Nd(0)$ corresponds to actual (t=0) calculated according to the equation $= \{[(^{143}Nd/^{144}Nd)_{am}/0.512638] - 1\}*10^4$, where $^{143}Nd/^{144}Nd_{CHUR} = 0.512638$ (Hamilton et al. 1983). $f_{Sm/Nd} = \{[(^{147}Sm/^{144}Nd)_{am}/0.1967)] -1\}$, where $^{147}Sm/^{144}Nd_{CHUR} = 0.1967$ (Hamilton et al. 1983). Average $^{143}Nd/^{144}Nd$ ratio for the standard JNDi since January-October/2012 = 0.512100 ± 0.000008. Sm and Nd contents (in ppm) determined by isotope dilution (ID).
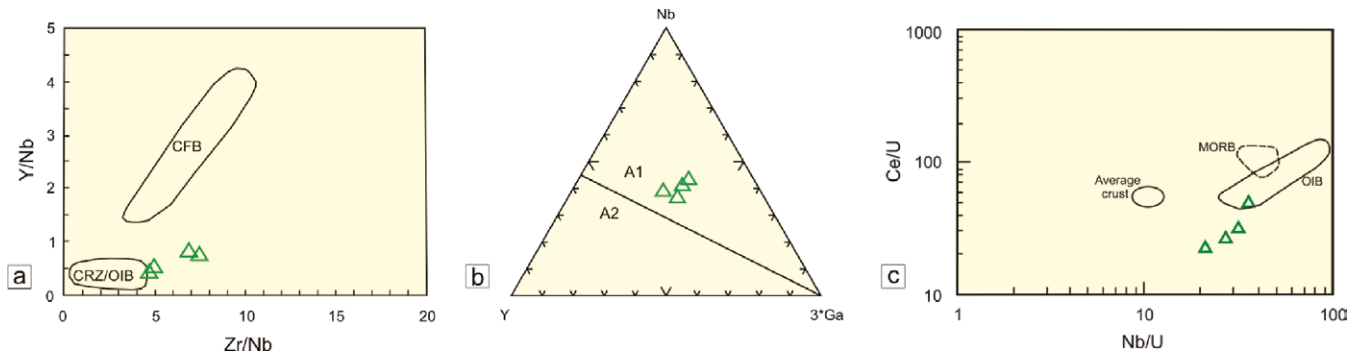

Figure 7: a) Y/Nb vs. Zr/Nb plot. The CRZ/OIB and CFB fields represent continental rift zone, oceanic island alkali basalts and continental flood basalts according to Wilson (1989); b) Y-Nb-Ga diagram (Eby 1992). A1 represents differentiates of magmas derived from mantle sources like those of oceanic-island basalts but emplaced in continental rifts or during intra-plate magmatism, A2 represents magmas derived from continental crust or under-plated continental crust that had been through a cycle of continent-continent collision or island-arc magmatism; c) Nb/U vs. Ce/U variation diagram. Oceanic island basalt (OIB), mid-oceanic ridge basalt (MORB), and average crust data are from Hofmann et al. (1986) in Gharib et al. (2012). Trace elements in ppm. Unfilled triangle: La Aguadita Trachyte.

magmatic sources (McDonough 1990). The studied trachyte has high Nb/U and Ce/U average ratios of 28.7 and 31.7, respectively. In the Nb/U vs. Ce/U diagram (Fig. 7c) the samples fall outside but close to the OIB field, slightly shifted toward the average continental crust. The Th/Nb ratio is also an index of the contribution of the continental crust material during the magmatic evolution. The Th/Nb ratios of La Aguadita Trachyte ranging from 0.22 to 0.35 are very high compared with the corresponding mantle value (≈ 0.07, Pin et al. 1992), suggesting possible crustal contamination. This crustal contamination is consistent with positive K, Rb and REE (La, Ce, Nd) anomalies, which in concordance with the positive but relatively low εNd value (+2.6) could indicate that the trachyte was derived from a mantle source with some degree of crustal contamination.

CONCLUSIONS

La Aguadita Trachyte is a new exponent of the Triassic volcanic activity in Sierra de Valle Fértil, Western Sierras Pampeanas. The discovery of this trachyte expands the number of outcrops attributed to the Triassic alkaline magmatism known in the area, and confirms the regional extent of the volcanic event.

The geochemical signature showed by La Aguadita Trachyte is typical of intraplate magmatism originated in an extensional tectonic regime. Moreover, the fractionated REE pattern of the trachyte is representative of a melt derived from a dominant mantle source (εNd = +2.6). The negative Ba, Sr, TiO_2, P_2O_5 and Eu anomalies, and the gradual decrease in LREE, confirm the important role of fractional crystallization during the magmatic evolution of this rock. It has a narrow variation range of Zr/Nb, low Y/Nb, and high Nb/La ratios resembling OIB signature,

which evolve from asthenospheric mantle source. Such mantle source would have been subjected to fractional crystallization processes to yield La Aguadita Trachyte. On the other hand, the Th/Nb ratio (0.22 - 0.35), low but positive εNd values, coupled with trace element data, would support the participation of a crustal component during ascent and crustal emplacement.

Alkaline volcanic rocks from Sierra de Valle Fértil are closely associated in space and time. They belong to the olivine alkali-basalt suite which represents an important crystal fractionation series. Consequently, La Aguadita Trachyte would be derived from a mantellic source that evolved by feldspar fractionation coupled with slightly crustal component.

Moreover, the obtained age of (218 ± 7 Ma), suggests that igneous activity related to extensional tectonics could have begun in the Lower Triassic and continued until at least the Upper Triassic. The ra-

diometric age and the petrographic, geochemical and tectonic features of this lithology, are consistent with alkaline magmatism generated in an intraplate continental environment during the process of rifting that affected the Western Sierras Pampeanas region.

REFERENCES

Cabanis, B. and Lecolle, M. 1989. Le diagramme La/10-Y/15-Nb/8: un outil pour la discrimination des séries volcaniques et la mise en evidence des processus de mélange et/ou de contamination crustales. Comptes Rendus de l'Académie des Sciences de Paris, Série 2, 309: 2023-2029.

Casquet, C., Rapela, C.W., Pankhurst, R.J., Baldo, E., Galindo, C., Fanning, C.M. and Dahlquist, J. 2012. Fast sediment underplating and essentially coeval juvenile magmatism in the Ordovician margin of Gondwana, Western Sierras Pampeanas, Argentina. Gondwana Research 22: 664-673.

Castro de Machuca, B., Pontoriero, S., Conte-Grand, A., Morata, D., López, M.G. and Domínguez, J.P. 2012. New finding of peralkaline volcanism in the eastern margin of the Sierra de Valle Fértil, Western Sierras Pampeanas, NW Argentina. Proceedings of the 34th International Geological Congress 2012, Abstract: 485. Brisbane, Australia. CD-ROM edition.

Cuerda, A.J., Cingolani, C., Varela, R. and Schauer, O.C. 1984. Descripción geológica de la Hoja 19d-Mogna, provincia de San Juan. Servicio Geológico Nacional, Boletín 192, 86 p., Buenos Aires.

Curriea, B.S., Colombi, C., Tabor, N.J., Shipmand, T.C. and Montañez, I.P. 2009. Strati-graphy and architecture of the Upper Triassic Ischigualasto Formation, Ischigualasto Provincial Park, San Juan, Argentina. Journal of South American Earth Sciences 27: 74-87.

Dahlquist, J.A., Alasino, P.H., Eby, N., Galindo, C. and Casquet, C. 2010. Fault controlled Carboniferous A-type magmatism in the proto-Andean foreland (Sierras Pampeanas, Argentina): Geochemical constraints and petrogenesis. Lithos 115: 65-81.

Dahlquist J.A., Alasino P.H. and Bello C. 2014. Devonian F-rich peraluminous A-type magmatism in the proto-Andean foreland (Sierras Pampeanas, Argentina): geochemical constraints and petrogenesis from the western-central region of the Achala batholith. Mineralogy and Petrology 108: 391-417.

Davidson, J. P. 1987. Crustal contamination versus subduction zone enrichment: examples from the Lesser Antilles and implications for mantle source compositions of island arc volcanic rocks. Geochimica et Cosmochimica Acta 51: 2185-2198.

Deer W.A., Howie R.A. and Zussman, J. 1966. An introduction to the rock-forming minerals. Longman, 527 p., London

De Paolo, D.J. 1981. Neodymium isotopes in the Colorado Front Range and implications for crust formation and mantle evolution in the Proterozoic. Nature 291: 193-197.

Droop, G.T.R. 1987. A general equation for estimating Fe3+ concentrations in ferromagnesian silicates and oxides from microprobe analyses, using stoichiometric criteria. Mineralogical Magazine 51: 431-435.

Eby, G. N. 1992. Chemical subdivision of the A-type granitoids: petrogenetic and tectonic implications. Geology 20: 641-644.

Faure, G. and Powell, J.L. 1972. Strontium Isotope Geology. Springer-Verlag, Berlin, Heidelberg, 188 p., New York.

Furque, G.; González, P. and Caballé, M. 1999. Hoja Geológica 3169-II San José de Jáchal. Provincias de San Juan y La Rioja. Servicio Geológico Minero Argentino, Instituto de Geología y Recursos Minerales, Boletín 259, 67 p., Buenos Aires.

Gharib, M.E., Obeid, M.A. and Ahmed, A.H. 2012. Paleozoic alkaline volcanism: geochemistry and petrogenesis of Um Khors and Um Shaghir trachytes of the central Eastern Desert, Egypt. Arabian Journal of Geosciences 5: 53-71.

Hamilton, P.J., O'Nions, R.K., Bridgwater, D. and Nutman, A. 1983. Sm-Nd studies of Archaean metasediments and metavolcanics from West Greenland and their implications for the Earth's early history. Earth and Planetary Sciences Letters 62: 263-272.

Irvine, T.N. and Baragar, W.R.A. 1971. A guide to the chemical classification of the common volcanic rocks. Canadian Journal of Earth Sciences 8: 523-548.

Kozlovsky, A.M., Yarmolyuk, V.V., Kovalenko, V.I., Savatenkov, V.M. and Velivetskaya, T.A. 2007. Trachytes, comendites, and pantellerites of the Late Paleozoic bimodal rift association of the Noen and Tost Ranges, Southern Mongolia: differentiation and contamination of peralkaline salic melts: Petrology 15: 240-263.

Leake, B.E. and 21 others 1997. Nomenclature of amphiboles: report of the Subcommittee on Amphiboles of the International Mineralogical Association, Commission on new minerals and mineral names. The Canadian Mineralogist 35: 219-246.

Leake, B.E., Wooley, A., Birch, W., Burke, E., Ferraris, G., Grice, J.D., Hawthorne, F.C., Kisch H., Krivovichev, V., Schumacher J.C., Stephenson N. and Whittaker, E. 2003. Nomenclature of amphiboles: additions and revisions to the International Mineralogical Association's 1997 recommendations. Canadian Mineralogist 41: 1355-1362.

Le Maitre, R., Bateman, P., Dudek, A., Keller, J., Lameyre, J., Le Bas, M., Sabine, P., Schmid, R., Sorensen, H., Streckeisen, A., Woolley, A. and Zanettin, B. 1989. In : Le Maitre, R.W. (ed.) A classification of igneous rocks and glossary of terms: Recommendations of the International Union of Geological Sciences Subcommission on the Systematics of igneous rocks. Blackwell, 193 p., Oxford.

Limarino, C.O., Page, S.M., Caselli, A., Net, L., Litvak, V., Pieters, P. and Lyons, P. 2008. Hoja Geológica 3166-I Chamical, Provincias de La Rioja y San Juan. Servicio Geológico Minero Argentino, Boletín 257, 77 p., Buenos Aires.

López, M.G., Domínguez, J.P., García, J.M. and Castro de Macuca, B. 2011. Traquiandesita basáltica Los Molles, Sierra de Valle Fértil, provincia de San Juan: consideraciones petrográficas y químicas. 5° Congreso Argentino de Estudiantes de Geología, Actas: 285-289,

San Juan. Editado en CD-ROM.

Macdonald, R. 1974a. Nomenclature and petrochemistry of peralkaline oversaturated extrusive rocks. Bulletin of Volcanology 38: 498-516.

Macdonald, R. 1974b. Tectonic settings and magma associations. Bulletin of Volcanology 38: 575-593.

Macdonald R., Davies G.R., Bliss C.M., Leat P.T., Bailey D.K. and Smith R.L. 1987. Geochemistry of high-silica peralkaline rhyolites, Nalvasha, Kenya Rift Valley. Journal of Petrology 28: 979-1007.

McDonough, W.F. 1990. Constraints on the composition of the continental lithospheric mantle. Earth and Planetary Sciences Letters 101: 1-18.

Martínez, R.N., Sereno, P.C, Alcober, O.A., Colombi, C.E., Renne, P.R., Montanez, I.P. and Currie, B.S. 2011. A basal dinosaur from the dawn of the dinosaur era in southwestern Pangaea. Science 331: 201-210.

Mirré, J.C. 1976. Descripción Geológica de la Hoja 19e, Valle Fértil, Provincias de San Juan y La Rioja. Servicio Geológico Nacional, Boletín 147: 70 p., Buenos Aires.

Nakamura, N. 1974. Determination of REE, Ba, Mg, Na and K in carbonaceous and ordinary chondrites. Geochimica et Cosmochimica Acta 38: 757-775.

Nohda, S. and Wasserburg, G.J. 1981. Nd and Sr isotopic study of volcanic rocks from Japan. Earth and Planetary Science Letters 52: 264-276.

Nono, A., Deruelle, B., Demaiffe, D. and Kambou, R. 1994. Tchabal Nganha volcano in Adamawa (Cameroon): petrology of a continental alkaline lava series. Journal of Volcanology and Geothermal Research 60: 147-78.

O' Halloran, D.A. 1985. Ras ed Dom migrating complex: A-type granites and syenites from the Bayuda Desert, Sudan. Journal of African Earth Sciences 3: 61-75.

Otamendi, J., Vujovich, G., de la Rosa J.D., Tibaldi, A., Castro, A., Martino, R.D. and Pinotti, L. 2009. Geology and petrology of a deep crustal zone from the Famatinian paleoarc, Sierras de Valle Fértil and La Huerta, San Juan, Argentina. Journal of South American Earth Sciences 27: 258-279.

Page, S., Limarino, C.O. and Caselli, A. 1997. Basaltos alcalinos en el Triásico de la Cuenca Ischigualasto-Villa Unión, provincias de La Rioja y San Juan. Revista de la Asociación Geológica Argentina 52: 202-208.

Panter, K. S., Kyle, P. R. and Smellie, J. R. 1997. Petrogenesis of a phonolite-trachyte succession at Mt. Sidley, Marie Byrd Land, Antarctica. Journal of Petrology 38: 1225-1253.

Pearce, J.A., Harris, N.B.W. and Tindle, A.G. 1984. Trace element discrimination diagrams for the tectonic interpretation of granitic rocks. Journal of Petrology 25: 956-983.

Pin, C., Cuesta, L. and Ibarguchi, J.I. 1992. Mantle-derived, Early Paleozoic A-type metagranitoids from the NW Iberian massif: Nd isotope and trace element constrains. Bulletin de la Societe Geologique de France 163: 483-494.

Ramos, V. and Kay, S. 1991. Triassic rifting and associated basalts in the Cuyo basin, central Argentina. In: Harmon, R. and Rapela, C. (eds.) Andean magmatism and its tectonic setting. Geological Society of America, Special Paper 265: 79-92, Boulder, Colorado.

Siivola, J. and Schmid, R. 2007. List of Mineral Abbreviations. Recommendations by the IUGS Subcommission on the Systematics of Metamorphic Rocks: Web version 01.02.07. www.bgs.ac.uk/scmr/home.html

Smith E., Isanchez A., Walker J.D. and Wang, K. 1999. Geochemistry of mafic magmas in the Hurricane volcanic field, Utah: implications for small- and large-scale chemical variability of lithospheric mantle. Journal of Geology 107: 433-448.

Steiger, R.H. and Jäger, E. 1977. Subcommission on geochronology: convention on use of decay constants in geo- and cosmochronology. Earth and Planetary Science Letters 36: 359-362.

Sun, S. and McDonough, W.F. 1989. Chemical and isotopic systematics of oceanic basalts: implications for mantle composition and processes. In: Saunders, A. D. and Norry, M. J. (eds), Magmatism in the Ocean Basins, Geological Society Special Publication 42: 313-345.

Uliana, M.A. and Biddle, K.T. 1988. Mesozoic-Cenozoic paleogeographic and geodynamic evolution of southern South America. Revista Brasileira de Geociencias 18: 172-190.

Wilson, M. 1989. Igneous Petrogenesis. A Global Tectonic Approach. Chapman & Hall, London, 466 p.

White J.C. and Urbanczyk, K.M. 2001. Origin of a silica-oversaturated quartz trachyte-rhyolite suite through combined crustal melting, magma mixing, and fractional crystallization: the Leyva Canyon volcano, Trans-Pecos Magmatic Province, Texas. Journal of Volcanology and Geothermal Research 11: 155-182.

Winchester, J.A. and Floyd, P.A. 1977. Geochemical discrimination of different magma series and their differentiation products using immobile elements. Chemical Geology 20: 325-343.

Wood, D. A. 1980. The application of a Th-Hf-Ta diagram to problems of tectonomagmatic classification and to establishing the nature of crustal contamination of basaltic lavas of the British Tertiary volcanic province. Earth and Planetary Science Letters 42: 77-97.